International
Science and Technology Journal
المجلة الدولية للعلوم والتقنية

Volume 24 العدد
January 2021 يناير

Green Synthesis and Characterization of Iron Oxide Nanoparticles Using *MenthaPiperita* Leaves Extract

Fatma Ali Shtewi* **Wedad Mohammed Barag** **Awatef Abdulsalam Tarroush**

Chemistry Department, Faculty of Science, Zawia University, Libya
***Correspondence Email address**: F.shtewi@zu.edu.ly

Abstract:

The green synthesis method of α-Fe_2O_3 nanoparticles has advantageous over other physical and chemical methods. In the present study, green synthesis of hematite (α-Fe_2O_3) nanoparticles was carried out via an eco-friendly method using aqueous ferric chloride solution ($FeCl_3.6H_2O$) as precursor and the aqueous extract of *Menthapiperita* leaves as a reluctant and stabilizer. The precursor salt solution and stabilizer agent were mixed in a 1:1 volume ratio at room temperature. The synthesized α-Fe_2O_3 nanoparticles were characterized by UV–VIS absorption spectroscopy, Fourier transform infrared spectroscopy (FTIR) and X-ray diffraction (XRD). The α-Fe_2O_3 nanoparticles showed absorbance peak at 430 nm region in the spectral analysis.As well as, the band gap energy of α-Fe_2O_3 nanoparticles determined from UV–Visible spectra with the help of Tauc plot was 2.602 eV. FTIR spectra confirmed the presence of poly phenols, which are responsible for the reduction of Fe^{3+} ions and efficient stabilization of α-Fe_2O_3 nanoparticles. The XRD result revealed that the average crystallite size of α-Fe_2O_3 nanoparticles was 8.8 nm. Furthermore, the mechanism of α-Fe_2O_3 nanoparticle formation has also been discussed.

Key-words**:** Hematite (α-Fe_2O_3) Nanoparticles, Green Synthesis Menthapiperita, Characterization, Mechanism.

الملخص :

طريقة الإصطناع الاخضر لجسيمات $\alpha-Fe_2O_3$ النانوية لها مميزات تفوق الطرق الفيزيائية والكيميائية الأخرى. في هذا البحث، تم إجراء التخليق الأخضر لجسيمات الهيماتيت النانوية ($\alpha-Fe_2O_3$) عبر طريقة صديقة للبيئة باستخدام محلول كلوريد الحديديك المائي ($FeCl_3.6H_2O$) كبادئ والمستخلص المائي لأوراق النعناع كعامل مختزل ومثبت. تم خلط محلول الملح البادئ والعامل المختزل بنسبة حجمية 1:1 عند درجة حرارة الغرفة. تم تشخيص جسيمات اكسيد الحديد الثلاثي النانوية $\alpha-Fe_2O_3$ بواسطة التحليل الطيفي لامتصاص الأشعة فوق البنفسجية، مطيافية الأشعة تحت الحمراء (FTIR) وحيود الأشعة السينية (XRD).أظهرت جسيمات أكسيد الحديد الثلاثى $\alpha-Fe_2O_3$ النانوية قمة امتصاص عند 430 نانومتر في التحليل الطيفي. بالإضافة إلى ذلك ، كانت طاقة فجوة النطاق لجسيمات $\alpha-Fe_2O_3$ النانوية المحددة من الطيف المرئي للأشعة فوق البنفسجية بمساعدة مخطط Tauc هي 2.602 الكترون فولت. كشف طيف FTIR عن وجود البوليفينولات المسؤولة عن إختزال أيونات Fe^{3+} والتثبيت الفعال لجسيمات $\alpha-Fe_2O_3$ النانوية. كشفت نتيجة XRD أن متوسط الحجم البلوري للجسيمات النانوية $\alpha-Fe_2O_3$ كان 8.8 نانومتر. علاوة على ذلك تمت أيضًا مناقشة آلية تكوين جسيمات $\alpha-Fe_2O_3$ النانوية.

1. Introduction:

Nanotechnology is a multidisciplinary branch of science that includes various areas of science and technology, including biomedicine, pharmaceutics, environmental, science, and others. Nanotechnology is one of the most exciting fields which are used to describe the formation and utilization of materials with structural features between those of atoms and bulk materials with a minimum of one dimension in the nano range. Nanoparticles are the simplest form of structures with sizes in the range between almost 1 and 100 nanometers. Nanotechnology and nanoparticles based products and applications have increased nowadays due to biological effectiveness. Furthermore, it is well known that inorganic nanomaterials are good antimicrobial agents [1]. Nanoparticles exhibit an intensive range of properties such as lower melting points, higher surface area, mechanical strength, specific optical properties specific magnetizations, and biological activity [2, 3] which is different from that of their bulk materials. Processes used for metal oxide nanoparticle synthesis are chemical, physical, and a recently developed biological method.

Iron oxide nanoparticles (IONPs) have attracted much concern owing to their unique properties, such as super paramagnets, surface-to-volume ratio, greater surface area, a propensity to agglomerate and easy separation methodology. Common kinds of iron oxide are hematite (α-Fe_2O_3), maghemite (γ-Fe_2O_3) wustite (FeO) and magnetite (Fe_3O_4). Recently, nano-crystalline α-Fe_2O_3 is one of the most useful materials for photocatalytic and photo-electrochemical applications due to its narrow band gap (2.0–2.2 eV), which could collect up to 40 % of the solar spectrum energy [4]. The α-Fe_2O_3 nanoparticles exhibit great stability in aqueous solutions and good magnetic properties. The crystal structure of hematite α-Fe_2O_3 is rhombohedral system and it shows a weak ferromagnetism at 300K. The hematite α-Fe_2O_3 is an n-type semiconductor which has attracted substantial interest because of their potential applications, including pigments, gas sensors, an anode material, optical devices, medicine applications and it used as catalysis [5-8]. It can also be used as a starting material for the synthesis of magnetite (Fe_3O_4) and maghemite (γ-Fe_2O_3), which have been intensively pursued for both fundamental scientific interest sand technological applications in the last few decades [9]. A various available methods have been developed for synthesis ofα-Fe_2O_3nano-particles, including hydro thermal synthesis [10], polyol method [11], sol–gelmethod [12], ultrasonic spray pyrolysis [13], chemical vapor deposition [14], co-precipitation [15] and pulsed laser deposition [16]. However, these methods are usually expensive and labor-intensive and are potentially hazardous to the environment and living organisms. Therefore, using the phytochemicals present in plants as bio-reductants is attaining a greater impetus. Different parts of plant materials such as leaf extracts, fruit, bark, fruit, peels, root, and callus have been focused on the synthesis of metallic nanoparticles [17].

The chemical and physical methods for nanoparticles synthesized are suffering from drawbacks. In this work, we successfully synthesized α-Fe_2O_3 nanoparticles through a rapid, simple, and economical route, without any hazardous chemicals as reducing or stabilizing agents. Moreover, the use of water as a solvent for the preparation of the extract is considered to be the cheapest and greenest method for the production ofα-Fe_2O_3 nanoparticles. Among several plants, *Menthapiperita* Leaves (Lamiaceae family) is commonly known as*peppermint*. The *Peppermint* with vernacular names of “nana”, a plant is one of the herbs most extensively used worldwide, with an extended history as a medical plant. It contains large amounts of polyphenols that are biodegradable and soluble in water at room temperature and have molecules carrying hydroxyl groups that can be used for the reduction and the stabilization of the nanoparticles [18, 19]. The abbreviations used throughout the paper are described in Table 1.

Table (1): List of abbreviations used throughout the paper.

Abbreviations	Definitions
UV–vis	Ultraviolet–visible
FTIR	Fourier transform infrared spectroscopy
XRD	X-ray diffraction
NPs	Nanoparticles
FWHM	The full width at half maximum
Pos. [°2 Th.]	Position [^{o}2 Theta]

2. Materials and Methods

Fresh leaves of *Menthapiperita* plant were collected from Az-Zāwiyah, Libya. Ferric chloride hexahydrate ($FeCl_3.6H_2O$) was purchased from Sigma Aldrich. The α-Fe_2O_3 nanoparticles were synthesized by the green synthesis method using ferric chloride as a precursor and plant extract as reducing and capping agents. The crystal structure of the sample was analyzed by using the XRD-6100 diffractometer (Shimadzu), and the patterns were recorded with Copper Kα radiation (λ=1.54060 Å). Molecular analysis of the sample was performed by Fourier transform infrared (FT-IR) spectroscopy using IRAffinity-1S(Shimadzu) spectrometer, recorded in the wavenumber range of 500–4,000 cm^{-1}. The maximum optical absorption of the sample was characterized by UV-Visible Spectroscopy (JASCO V 670), in the range of 200-800nm. The optical characteristics of α-Fe_2O_3 nanoparticles were analyzed from ultraviolet-visible (UV-vis) spectrometer measurement. The optical band gap was determined using Touch's plot method hν versus $(\alpha h\nu)^{1/2}$, where α and hν denote the optical absorption coefficient and photon energy respectively.

2.1 Plant Extract Preparation:

A 20 g of *Menthapiperita* leaves were washed thoroughly with tap water and then rinsed with distilled water until no foreign material remained. The leaves were finely cut and were boiled for 15 min with 100 ml of distilled water in 500-ml Erlenmeyer flask. The aqueous extract was filtered through What man No. 1 filter paper.

2.2 Synthesis of Hematite α-Fe_2O_3 nanoparticles:

Hematite α-Fe_2O_3 nanoparticles were synthesized by adding freshly prepared leaves extract to $FeCl_3.6H_2O$ solution (0.1 M) in a 1:1 volume ratio. The immediate color change of the ferric chloride solution from light brown to black was observed and confirmed by spectrophotometric determination. The formation of α-Fe_2O_3 nanoparticles was marked by the appearance of the black color. The α-Fe_2O_3nanoparticles were separated by centrifuging at 3000 rpm for 15 minutes, and dried in the open air for 24 hr. All the following procedures were performed at room temperature and under atmospheric pressure.

3. Results and Discussion

3.1 UV–Vis spectroscopy:

The formation of hematite α-Fe_2O_3 nanoparticles was observed by UV–vis absorption spectroscopy (Figure 1). Initially, the leaves extract had a yellow color and showed higher absorption peaks at the region 200 to 350 nm. It indicates that the leaves extract had free phytochemicals. After the addition of leaves extract to ferric chloride solution, a black-colored colloidal solution was formed. The spectra of the black-colored colloidal solution show the disappearance of strong absorption peaks at the region 200 to 350 nm and emerge a sharp peak at higher wavelengths region at 430 nm suggesting the formation of α-Fe_2O_3 nanoparticles. This finding is in agreement with previous reports for the green synthesis of α-Fe_2O_3nanoparticles using both *Pomegranate* seeds and *Ailanthus excels* leaves extracts [20,21].

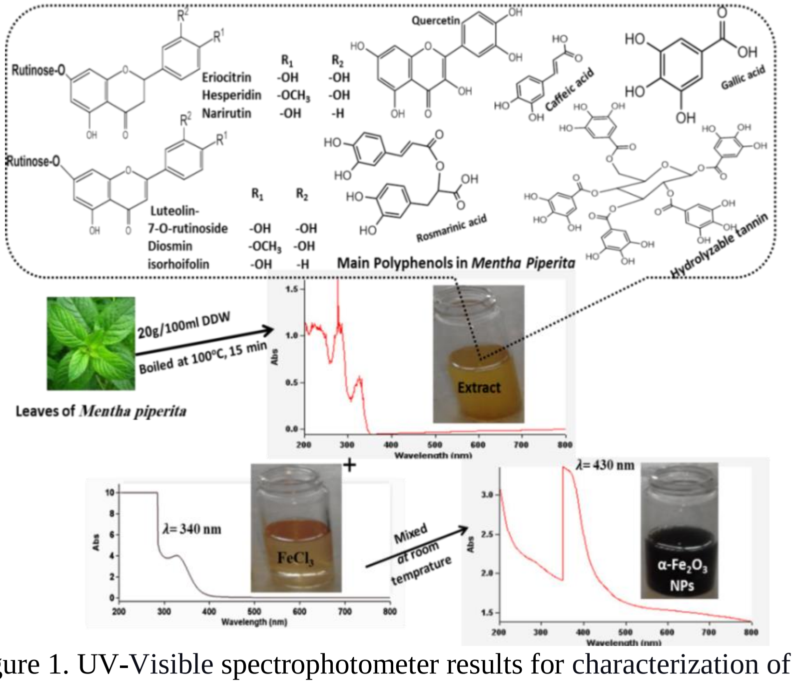

Figure 1. UV-Visible spectrophotometer results for characterization of α-Fe_2O_3 nanoparticles

3.2 Band gap energy:

Optical properties of nanoparticles give information about physical properties; such as band gap energy, band structure and optically active defects. The band gap energy of α-Fe_2O_3 nanoparticles was determined from the UV analysis with the help of Tauc plot. The optical band gap of the produced nanoparticles is calculated using the Tauc'sequation (1):

$\alpha h\nu = A(h\nu - E_g)^{1/2}$ ……………………… (Eq. 1)

Where: α is the absorption coefficient, E_g is the band gap energy, A is constant and $h\nu$ is the photon energy in eV.

Figure 2 shows $(\alpha h\nu)^2$ versus $h\nu$ plot of absorption spectrum of colloidal solution of α-Fe_2O_3 nanoparticles. The obtained direct band gap value of α-Fe_2O_3 nanoparticles was determined from the intercept of the straight line with the $h\nu$-axis. The band gap value is found to be 2.602 eV, which is in good agreement with the reported value(2.67 eV) of α-Fe_2O_3 nanoparticles by literatures [22, 23]. Besides, the observed value is higher than the standard value of α-Fe_2O_3 (1.9 eV–2.2 eV) [4], due to the decrease in the particle size (8.8 nm) of hematite is responsible for increasing the optical band gap [24].

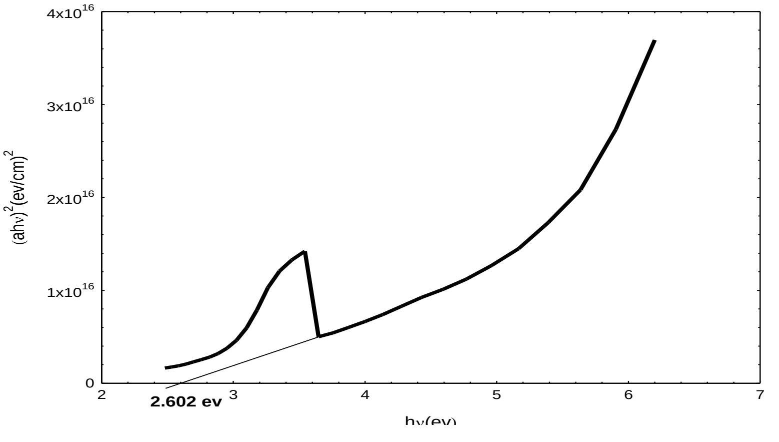

Figure 2. Band gap energy of α-Fe_2O_3 nanoparticles

3.3 FT-IR Spectroscopy:

FT-IR measurements were employed to investigate the possible functional groups responsible for the reduction of the metal precursors and the formation of α-Fe_2O_3 nanoparticles. The comparison of FT-IR spectra between pure *Menthapiperita* leaf and its complexation with Fe^{3+} ions are shown in Figure 3. The infrared spectra of the dried *Menthapiperita* leaves show the absorption peaks at 1253.69 and 1014.85 cm^{-1} are ascribed for the C-O-C and C-O-H vibrations of the phenolic group. Also, the two small bands at 1416.17 cm^{-1} and 1517.47 cm^{-1} can be related to symmetric and asymmetric stretching vibrations of COO^- group. The band observed at 1601.29 cm^{-1} is attributed to the C=C stretching vibrations of the aromatic ring, which belongs to the polyphenols (e.g., flavonoids and tannins) [18]. Moreover, a small peak at 1730.08 cm^{-1} is correspond to the C=O stretching vibration, indicates that an ester bond is formed between two galloyl groups, which confirms the *presence* of hydrolysable tannins [25, 26]. The sharp peaks at 2919.45 cm^{-1} and 2850.56 cm^{-1} are attributed to asymmetric and symmetric C-H stretching mode of aliphatic hydrocarbon chains. The broad band at 3275.08 cm^{-1} is representing the O–H stretching vibration of the polyphenolic compounds, which is an indication of the strong hydrogen bonding [27]. These functional groups prove the presence of polyphenols in *Menthapiperita*, which might act as reducing and stabilizing agents in the α-Fe_2O_3 nanoparticles synthesis. The FTIR spectra reveal that observed bands for functionalized α-Fe_2O_3 nanoparticles (figure 3b) are similar to those obtained for *Menthapiperita* (figure 3a) with a slight shift. However, the absorption correspond to the C=O stretching vibration is shifted to 1700.61 cm^{-1}, which was attributed to the binding of a C=O group with the nanoparticles. Furthermore, the band involving O-H vibration at 3275.08 cm^{-1} of the polyphenolic compounds is shifted to lower wave number in the region between 2986.2 cm^{-1} and 3357.7 cm^{-1}, hence showing deprotonation of the -OH groups and coordination to Fe^{3+} ions [20]. Finally, appearance of the sharp absorption bands at 587.85, 566.86 and 543.88 cm^{-1} in the spectrum of α-Fe_2O_3 nanoparticles are attributed to the Fe–O stretching vibration [28, 29, 30].

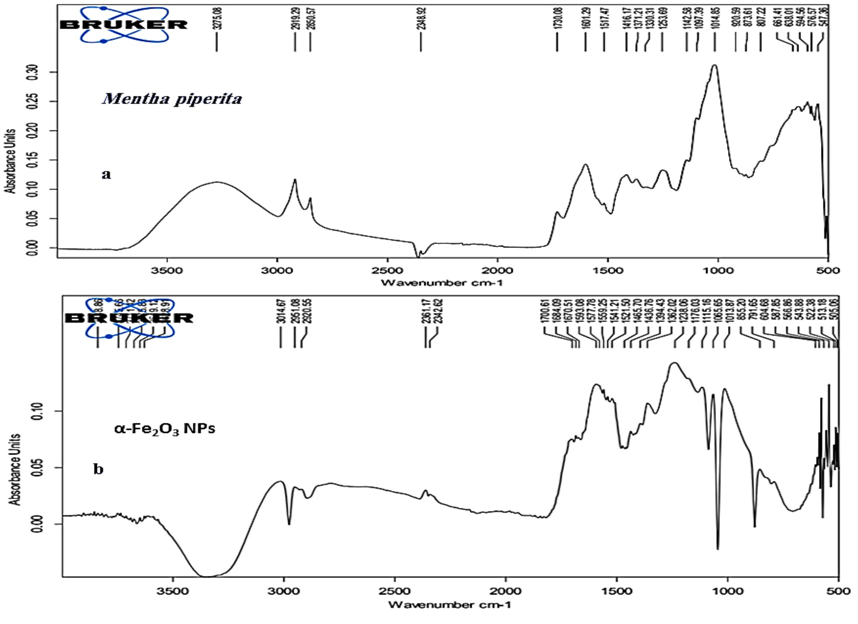

Figure 3. FT-IR Spectra of (a) the dried *Menthapiperita* leaves and (b) α-Fe_2O_3 nanoparticles

3.3 X-ray Diffraction (XRD):

Figure 4 shows the XRD pattern of α-Fe_2O_3 nanoparticles. It was observed that the XRD pattern is like an amorphous pattern and it could be said that the sample is nano crystalline sized iron oxide particles. The XRD patterns of the sample show broad peaks, which clearly indicates that the sample is nano crystalline. In addition, the peaks are broad due to the nano size effect [30]. There are three distinct diffraction peaks with $2\theta = 27.71°$, $35.86°$, and $56.6°$ are observed, which indicates the formation of α-Fe_2O_3 nanoparticles. The broad peak at $2\theta = 27°$ can be recognized as organic components from leaf extract of *Menthepiperita*, which are responsible for stabilizing of nanoparticles, as well as consistent

International
Science and Technology Journal
المجلة الدولية للعلوم والتقنية

Volume 24 العدد
January 2021 يناير

المجلة الدولية للعلوم والتقنية
International Science and Technology Journal
ISTJ

with the FT-IR results. The diffraction peak at 2θ of 35.86° and 56.6° indicates the presence of α-Fe_2O_3, as well as consistent with the FT-IR result. The Figure 4 does not show all the peaks belongs to α-Fe_2O_3 nanoparticles, due to the presence of bioactive compounds from *Menthapiperita* leaves extract, or because of the α-Fe_2O_3 nanoparticles were prepared at room temperature and may also be due to a higher concentration of precursor salt. Thus, reported researches carried out calcined at high temperature to improve the crystallinity of α-Fe_2O_3 NPs, where at higher temperatures the crystallinity of the α-Fe_2O_3 NPs increases [31, 32, 33]. Moreover, another study showed that the reaction time playing a very important role in the clarity of the peaks of the XRD pattern. As the reaction time increases, the crystallinity of the hematite α-Fe_2O_3 nanoparticles increases [34].

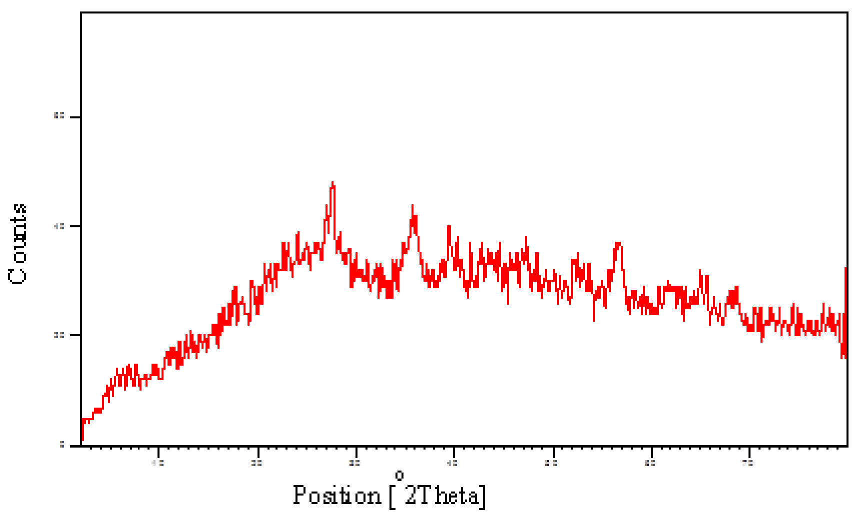

Figure 4. XRD pattern of α-Fe_2O_3 nanoparticles

The average crystallite size of the α-Fe_2O_3 NPs is calculated by using Debye–Scherrer's equation for 2θ= 35.86° as shown in the Equation (2) and Table (2):

$D = \frac{0.9 \times \lambda}{\beta \times \cos\theta}$.......................... (Eq. 2)
Where: 'λ' is wave length of X-Ray (0.154(nm)), 'β' is FWHM (full width at half maximum), 'θ' is the diffraction angle and 'D' is particle diameter size. The average crystallite size of the α-Fe_2O_3 NPs was 8.8 nm.

Table 2. X-ray diffraction peak list of α-Fe_2O_3 nanoparticles.

Pos. [°2Th.]	FWHM [°2Th.]	d-spacing [Å]
27.7149	0.4330	3.21885
35.8652	0.9446	2.50387
56.6130	1.1520	1.62446

$$\beta = \frac{\text{FWHM} \times \pi}{180} = \frac{0.9446 \times 3.14}{180} = 0.01648$$

$$D = \frac{0.9 \times \lambda}{\beta \times \cos\theta} = \frac{0.9 \times 0.154\, nm}{0.01648 \times 0.9514} = 8.8\, nm$$

3.4 Plausible Mechanism of α-Fe_2O_3 nanoparticles:

Menthapiperita leaves is known for having several polyphenols include phenolic acids, flavonoids (eriocitrin, narirutin, hesperidin, luteolin-7-O-rutinoside, isorhoifolin, diosmin, 5,7-dihydroxycromone-7-O-rutinoside), tannins and saponins as active substances [35, 36]. Although the mechanistic details of the biosynthesis processes are currently unclear, a range of mechanisms have been proposed to explain the formation of NPs. However, the exact mechanism of the synthesis process remains challenges, thus providing opportunities for further study. A plausible formation mechanism of the α-Fe_2O_3 nanoparticles from *Menthapiperita* is schematically presented in (Scheme 1) offering that polyphenols serve as a reducing and stabilizing agent. The

Menthapiperita leaf extract contains a high content of polyphenol as tannins (234.06 mg/g) with plenty of phenolic–OH of galloyl groups [37]. These functional groups can form a strong complex with Fe^{3+} ions, Furthermore, the hydroxyl groups of polyphenolic compounds are deprotonate and act to reduce the Fe^{3+} ions. The deprotonation of the hydroxyl groups of the polyphenols was confirmed by the IR spectra. Accordingly, the Fe^{3+} ions oxidized the hydroxyl groups into carbonyl groups in the reduction reaction as Fe^{3+} is reduced to Fe^0 NPs [38] and are subsequently oxidized by atmospheric oxygen or water resulting in α-Fe_2O_3 nanoparticles.

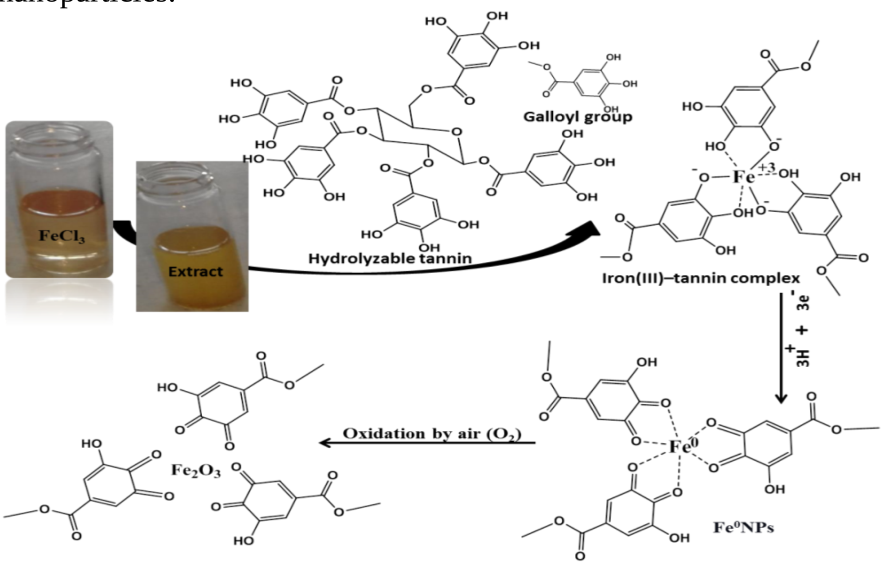

Scheme 1. Plausible complexation and reduction for the formation mechanism of α-Fe_2O_3 nanoparticles by galloyl groups of tannin

4. Conclusion:

In summary, the green synthesis method has merits over other physical and chemical methods, are easily available starting materials, inexpensive and procedure is easy to carry out any laboratory, use of toxic reagent is avoided and pollution. The green synthesis route had been used to synthesis α-Fe_2O_3 nanoparticles using *Menthapiperita* leaves extract. The FT-IR spectra demonstrated the presence of a polyphenolic compounds in the extract (mainly tannins) could be probably responsible for the reduction process through the hydroxyl groups and binding to the α-Fe_2O_3 nanoparticles through the carbonyl groups. Furthermore, the optical direct band gap energy of the α-Fe_2O_3 NPs determined from the Tauc plot was 2.602 eV. The XRD result illustrated that the average crystallite size of the α-Fe_2O_3nanoparticles was 8.8 nm. This eco-friendly method can potentially be employed in various areas, including pharmaceuticals, cosmetics, foods, and medical applications. Finally, other properties and applications of this type of material should be explored in future studies.

Acknowledgements:

Authors are grateful to the Department of Chemistry Zawia University, Libyan Petroleum Institute at Tripoli, Polymer Research Center at Tripoli and the National Center for Medical Research at Zawia for approving and facilitating this work. The authors also appreciate Prof.Dr. Hussain Ibrahim Alarabi (Professor Chemistry Department, Zawia University) for helpful discussions and advice during the development of the work.

References:

[1] K. Chatterjee, S. Sarkar, K. J. Rao, S. Paria, Core/shell nanoparticles in biomedical applications, Advances in colloid and interface science 209 (2014) pp. 8-39.

[2] L. R. Hirsch, R. J. Stafford, J. A. Bankson, S. R. Sershen, B. Rivera, R. E. Price, J. L. West, Nanoshell-mediated near-infrared thermal therapy of tumors under magnetic resonance guidance, Proceedings of the National Academy of Sciences 100(23) (2003) pp. 13549-13554.

[3] S. Saif, A. Tahir, Y. Chen, Green synthesis of iron nanoparticles and their environmental applications and implications, Nanomaterials 6(11) (2016) pp. 209.

[4] M. Alagiri, S. B. A. Hamid, Green synthesis of α-Fe_2O_3 nanoparticles for photocatalytic application, Journal of Materials Science: Materials in Electronics 25(8) (2014) pp. 3572-3577.

[5] D. Walter, Characterization of synthetic hydrous hematite pigments, Thermochimicaacta 445(2) (2006) pp. 195-199.

[6] C. Wu, P. Yin, X. Zhu, C. OuYang, Y. Xie, Synthesis of hematite (α-Fe_2O_3) nanorods: diameter-size and shape effects on their applications in magnetism, lithium ion battery, and gas sensors, The Journal of Physical Chemistry B 110 (36) (2006) pp. 17806-17812.

[7] X. Gou, G. Wang, J. Park, H. Liu, J. Yang, Monodisperse hematite porous nanospheres: synthesis, characterization, and applications for gas sensors, Nanotechnology 19 (12) (2008) pp. 125606.

[8] T. Ohmori, H. Takahashi, H. Mametsuka, E. Suzuki, Photocatalytic oxygen evolution on α-Fe_2O_3 films using Fe^{3+} ion as a sacrificial oxidizing agent, Physical Chemistry Chemical Physics 2(15) (2000) pp. 3519-3522.

[9] W. Wu, Z. Wu, T. Yu, C. Jiang, W. S. Kim, Recent progress on magnetic iron oxide nanoparticles: synthesis, surface functional strategies and biomedical applications, Science and technology of advanced materials 16 (2015), pp. 23501-23543.

[10] F. Wang, X. F. Qin, Y. F. Meng, Z. L. Guo, L. X. Yang, Y. F. Ming, Hydrothermal synthesis and characterization of α-Fe_2O_3 nanoparticles, Materials science in semiconductor processing 16 (3) (2013) pp. 802-806.

[11] H. Mansour, H. Letifi, R. Bargougui, S. De Almeida-Didry, B. Negulescu, C. Autret-Lambert, S. Ammar, A. Gadri, Structural, optical, magnetic and electrical properties of hematite (α-Fe_2O_3) nanoparticles synthesized by two methods: polyol and precipitation. Applied Physics A 123(12) (2017) pp. 787.

[12] K. Raja, M. M. Jaculine, M. Jose, S. Verma, A. A. M.

Prince, K. Ilangovan, S. J. Das, Sol–gel synthesis and characterization of α-Fe_2O_3 nanoparticles, Superlattices and Microstructures 86 (2015) pp. 306-312.

[13] B. K. Ozcelik, C. Ergun, Synthesis and characterization of iron oxide particles using spray pyrolysis technique, Ceramics International 41(2) (2015) pp. 1994

[14] N.A. Arzaee, M.F.M. Noh, A. Ab Halim, M.A.F.A. Rahim, N.A. Mohamed, J. Safaei, A. Aadenan, S.N.S. Nasir, A.F. Ismail, M.A.M. Teridi, Aerosol-assisted chemical vapour deposition of α-Fe_2O_3 nanoflowers for photoelectrochemical water splitting, Ceramics International, 45(14) (2019) pp.16797-16802.

[15] M. Farahmandjou, F. Soflaee, Synthesis and characterization of α-Fe_2O_3 nanoparticles by simple co-precipitation method, Physical Chemistry Research 3(3) (2015) pp. 191-196.

[16] T. M. N. Thai, S. R. Kim, H. J. Kim, Synthesis of Fe_2O_3 polymorph thin films via a pulsed laser deposition technique, New Phys SaeMulli 64 (2014) pp. 252-255.

[17] A. Zambre, A. Upendran, R. Shukla, N. Chanda, K. Katti, C. Cutler, R. Kannan, K. V. Katti, Green Nanotechnology—a Sustainable Approach in the Nanorevolution. In Sustainable Preparation of Metal Nanoparticles: Methods and Applications, The Royal Society of Chemistry: London, UK (2012), pp. 144–156.

[18] S. R. Patil, R. S. Patil, A. G. Godghate, Menthapiperita Linn: Phytochemical, antibacterial and dipterianadulticidal approach, Int. J. Pharm. Pharm. Sci 8(3) (2016) pp. 352.

[19] P. Sujana, T. M. Sridhar, P. Josthna, C. V. Naidu, Antibacterial activity and phytochemical analysis of Menthapiperita L.(Peppermint) An important multipurpose medicinal plant, American Journal of Plant Sciences 4 (2013) pp. 77-83.

[20] I. Bibi, N. Nazar, S. Ata, M. Sultan, A. Ali, A. Abbas, K. Jilani, S. Kamal, F.M. Sarim, M. I. Khan, F. Jalal, Green

synthesis of iron oxide nanoparticles using pomegranate seeds extract and photocatalytic activity evaluation for the degradation of textile dye, Journal of Materials Research and Technology 8(6) (2019) pp. 6115-6124.

[21] H. M. Asoufi, T. M. Al-Antary, A. M. Awwad, Green route for synthesis hematite (α-Fe_2O_3) nanoparticles: Toxicity effect on the green peach aphid, Myzuspersicae (Sulzer). Environmental Nanotechnology, Monitoring & Management 9 (2018) pp. 107-111.

[22] P. Mallick, B. N. Dash, X-ray diffraction and UV-visible characterizations of α-Fe_2O_3 nanoparticles annealed at different temperature, J. Nanosci.Nanotechnol 3(5) (2013) pp. 130-134.

[23] P. Mallick, Influence of different materials on the microstructure and optical band gap of α-Fe_2O_3nanoparticles, Materials Science-Poland, 32(2) (2014) pp. 193-197.

[24] A. Lassoued, B. Dkhil, A. Gadri, S. Ammar, Control of the shape and size of iron oxide (α-Fe_2O_3) nanoparticles synthesized through the chemical precipitation method, Results in physics 7 (2017) pp. 3007-3015.

[25] J. Jeyasundari, P. S. Praba, Y. B. A. Jacob, V. S. Vasantha, V. Shanmugaiah, Green synthesis and characterization of zero valent iron nanoparticles from the leaf extract of Psidiumguajava plant and their antibacterial activity, Chemical ScienceReview and Letters 6(22) (2017) pp. 1244-1252.

[26] F. dos Santos Grasel, M. F. Ferrão, C. R. Wolf, Development of methodology for identification the nature of the polyphenolic extracts by FTIR associated with multivariate analysis, SpectrochimicaActa Part A: Molecular and Biomolecular Spectroscopy 153 (2016) pp. 94-101.

[27] V.C. Karade, S.B. Parit, V.V. Dawkar, R.S. Devan, R.J. Choudhary, V.V. Kedge, N.V. Pawar, J.H. Kim, A.D.

Chougale, A green approach for the synthesis of α-Fe_2O_3 nanoparticles from Gardenia resinifera plant and it's In vitro hyperthermia application, Heliyon 5(7) (2019) 20-44.

[28] J. Wang, G. Meng, K. Tao, M. Feng, X. Zhao, Z. Li, H. Xu, D. Xia, J. R. Lu, Immobilization of lipases on alkyl silane modified magnetic nanoparticles: effect of alkyl chain length on enzyme activity, Plo S one, 7(8) (2012) pp. 43-78.

[29] D. Manyasree, P. Kiranmayi, R. V. Ravi Kumar, Synthesis, characterization and antibacterial activity of iron oxide nanoparticles .Indo American Journal of Pharmaceutical Research 6(7) (2016) pp. 5992-5997.

[30] M. Seyedi, S. Haratian, J. V. Khaki, Mechanochemical Synthesis of Fe_2O_3 Nanoparticles, Procedia Materials Science 11 (2015) pp. 309-313

[31] S. TaghaviFardood, F. Moradnia, S. Moradi, R. Forootan, F. YekkeZare, M. Heidari, Eco-friendly synthesis and characterization of α-Fe_2O_3 nanoparticles and study of their photocatalytic activity for degradation of Congo red dye, Nanochemistry Research, 4(2) (2019) pp. 140-147.

[32] D. M. Yufanyi, , A. M. Ondoh, , J. Foba-Tendo, , K. J. Mbadcam, Effect of decomposition temperature on the crystallinity of α-Fe_2O_3 (Hematite) obtained from an Iron (III)-Hexamethylenetetramine Precursor, Am. J. Chem 5(1) (2015) pp. 1-9.

[33] M. Rincón Joya, J. Barba Ortega, J. O. D. Malafatti, E. C. Paris, Evaluation of Photocatalytic Activity in Water Pollutants and Cytotoxic Response of α-Fe_2O_3 Nanoparticles, ACS omega 4(17) (2019) pp. 17477-17486.

[34] S. P. Schwaminger, R. Surya, S. Filser, A. Wimmer, F. Weigl, P. Fraga-García, S. Berensmeier, Formation of iron oxide nanoparticles for the photooxidation of water: Alteration of finite size effects from ferrihydrite to hematite, Scientific reports 7(1) (2017) pp. 1-9.

[35] S. C. C. Trevisan, A. P. P. Menezes, S. M. Barbalho, É. L. Guiguer, Properties of menthapiperita: a brief review, World J Pharm Med Res *3* (1) (2017) pp. 309-13.

[36] O. R. Pereira, S. M. Cardoso, Overview on Mentha and Thymus polyphenols, Current Analytical Chemistry 9 (3) (2013) pp. 382-396.

[37] M. Akhbari, R. Hajiaghaee, R. Ghafarzadegan, S .Hamedi, M. Yaghoobi, Process optimisation for green synthesis of zero-valent iron nanoparticles using Menthapiperita, IET nanobiotechnol 13(2) (2018) pp. 160-169.

[38] S. Sebatini, S. Kalluri, A. A. Madhavan, Green synthesized α-Fe_2O_3 mesoporous network for heterogeneous Fenton oxidation of thiazine dye, Materials Letters: X 5 (2020) pp. 10-37.